

Bosonic Stimulation in the Formation of a Bose-Einstein Condensate

H.-J. Miesner, D. M. Stamper-Kurn, M. R. Andrews,
D. S. Durfee, S. Inouye, W. Ketterle

The formation of a Bose-Einstein condensate of a dilute atomic gas has been studied in situ with a nondestructive, time-resolved imaging technique. Sodium atoms were evaporatively cooled close to the onset of Bose-Einstein condensation and then suddenly quenched to below the transition temperature. The subsequent equilibration and condensate formation showed a slow onset distinctly different from simple relaxation. This behavior provided evidence for the process of bosonic stimulation, or coherent matter-wave amplification, crucial to the concept of an atom laser.

At low temperature, many properties of systems are determined by the quantum statistics of their constituents. For one type of particles, known as bosons, transition rates into a given quantum state are enhanced by the presence of other identical bosons in that state. Explicitly, if N bosons occupy a given state, the transition rates into that state are proportional to $(N + 1)$. This effect, known as Bose stimulation, is most familiar as the gain mechanism in an optical laser, where the presence of photons in the lasing mode stimulates the emission of more photons into it. Similarly, in the case of bosonic atoms, Bose stimulation can lead to matter-wave amplification and constitutes the gain mechanism of an atom laser, a device that creates a coherent beam of atoms by means of a stimulated process. The Bose-Einstein distribution function can be derived from Bose stimulation and detailed balance. In particular, a Bose-Einstein condensate is only stable because of the enhanced elastic scattering into the condensate. Bose-Einstein condensation (BEC) was recently observed in dilute atomic gases (1) and was used to realize an atom laser. Our first demonstration of an atom laser (2, 3) focused on the direct proof that atoms coupled out from a condensate were coherent. In this work, we consider the gain process by studying the formation of the condensate.

The theoretical description of BEC in weakly interacting dilute gases has a long history and has accounted for most of the experimental results (4, 5). In contrast, a full description of the dynamics of condensate formation has not yet been developed. Predictions for the time scale of condensation varied between infinite (6) and extremely short (7). The early prediction for infinite time was based on a Boltzmann equation; in this framework, the condensate fraction cannot grow from zero (6, 8, 9). Thus, a separate

process of nucleation had to be introduced with Boltzmann equations describing the dynamics only before (10) and after (11) the nucleation. Stoof suggested that a condensate nucleates in a short coherent stage (7, 9, 12) and then grows according to a kinetic equation. Kagan and collaborators discussed the formation of a quasi-condensate that, in contrast to a condensate, has phase fluctuations; they die out on a time scale that increases with the size of the system (13–16). In the thermodynamic limit, it would take infinite time to establish off-diagonal long-range order. Recently, a fully quantum mechanical kinetic theory for a Bose gas has been formulated and was used to model the formation process of the condensate (17).

The experimental realization of BEC certainly proved that condensates form within a finite time. Likewise, the observation of high-contrast interference between two condensates demonstrated that condensates develop long-range coherence in a finite time (2). However, a determination of the intrinsic time scales was not possible because the cooling was slow enough that the system stayed close to thermal equilibrium. Thus, the buildup of the condensate followed the externally controlled temperature and did not reveal the more rapid intrinsic dynamics of condensate formation. In the work presented here, we cooled the system to a temperature slightly above the phase transition and then suddenly created a nonequilibrium configuration of lower energy in order to observe the intrinsic relaxation toward a new condensed equilibrium.

The experimental setup for cooling to the onset of BEC was similar to our previous work. Sodium atoms were optically cooled and trapped and then transferred into a cloverleaf magnetic trap (18). Further cooling by radio frequency (rf) evaporation (19) was conducted with a trapping potential determined by the axial curvature of the magnetic field of $B'' = 125 \text{ G cm}^{-2}$, the radial gradient of up to $B' = 150 \text{ G cm}^{-1}$, and the bias field

of typically $B_0 = 1.5 \text{ G}$. Most of this study was performed with a weaker trap, where the magnetically trapped cloud was adiabatically expanded after evaporative cooling by reducing B' to 80 G cm^{-1} . In the strong (weak) trap the transition was reached after 26 s of evaporation at $1.5 \text{ } \mu\text{K}$ ($1 \text{ } \mu\text{K}$) with 2×10^7 (9×10^7) sodium atoms in the $F = 1$, $m_F = -1$ ground state. The atom clouds were cigar-shaped, with the long axis horizontal.

The temperature of the cloud was controlled by the final frequency of the rf sweep during evaporative cooling and was brought to slightly above the phase-transition temperature. A nonequilibrium situation was then created by concluding the evaporation with a fast sweep of the rf frequency, ramping down by 200 kHz in 10 ms. This sweep caused a sudden truncation of the wings of the spatial distribution, where atoms were resonantly spin-flipped to a nontrapped state. The final frequency of the sweep depended critically on drifts in the magnetic bias field B_0 on the order of 10 mG. Rapid “quenching” of the cloud into the BEC regime was essential to clearly observe the onset of condensate formation. After the rf sweep, the intrinsic dynamics of condensate growth was observed without any further cooling in a completely isolated system.

The condensate was directly observed by nondestructive phase-contrast imaging (20, 21) with the use of a vertical probe laser beam at a detuning of 1.7 GHz. A series of 18 images was taken (Fig. 1) by a charge-coupled device (CCD) camera in kinetics mode (21), allowing for a time-resolved measurement of the formation of single condensates. The probe laser power was

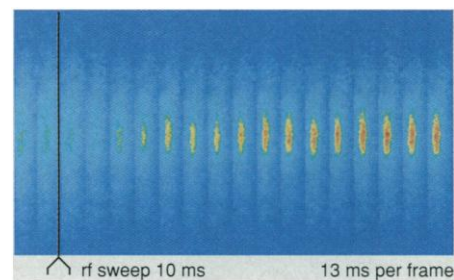


Fig. 1. Formation of a Bose-Einstein condensate. Shown is a sequence of 18 phase-contrast images of the same condensate taken in situ. The first two frames show a thermal cloud at a temperature above the transition temperature. The following 16 frames were taken after the cloud was quenched to below the BEC transition and show the growth of a condensate at the center of the cloud at 13-ms intervals. Note the decrease in the number of thermal atoms and their smaller width after the rf sweep. The column density of atoms is shown in false color: yellow to red marks the high density of the condensate. The length of the images is $630 \text{ } \mu\text{m}$.

Department of Physics and Research Laboratory of Electronics, Massachusetts Institute of Technology, Cambridge, MA 02139, USA.

chosen low enough that heating during the detection process was negligible. The initial and final equilibrium conditions were characterized by taking the first images before the sweep and the last three images 300 to 400 ms after. The ability to obtain real-time "movies" of the formation was used to overcome shot-to-shot fluctuations in initial conditions. The numbers of condensate and thermal atoms as well as the temperatures were extracted from one- and two-dimensional fits to the density distributions (Fig. 2). A bimodal function was fit to the density distribution with a Bose-Einstein distribution for the thermal fraction and an inverted parabola for the condensate density $n_0(\mathbf{r}) = n_0(0) - V(\mathbf{r})/\tilde{U}$. The latter is the solution of the nonlinear Schrödinger equation in the Thomas-Fermi approximation (22). Here, $V(\mathbf{r})$ denotes the trapping potential as a function of radial distance \mathbf{r} , and $\tilde{U} = 4\pi\hbar^2 a/m$ describes the interaction between the atoms of mass m , where \hbar is the Planck constant divided by 2π , and $a = 2.75$ nm is the scattering length. The temperatures were obtained by fits to the wings of the thermal fraction, and the absolute numbers of condensate atoms were determined from the axial length of the condensate assuming the Thomas-Fermi approximation. This result provided an accurate calibration for the phase-contrast signal. Condensates smaller than 10^5 atoms could not be discerned against the background of the thermal cloud.

Figure 3A shows a single-shot growth of the condensate. Equilibrium was reached within 200 ms after the rf sweep. Better statistics were obtained by averaging over

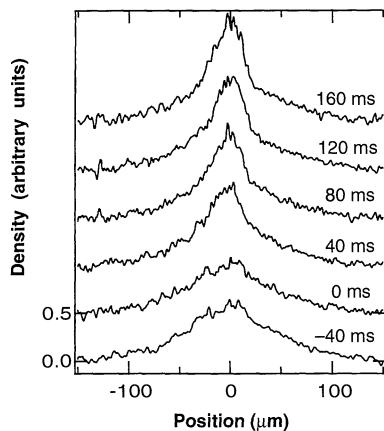


Fig. 2. Representative profiles of atom clouds during condensate formation. These are longitudinal cuts through the column densities obtained from phase-contrast images similar to those in Fig. 1. The rf sweep, which quenched the cloud, was applied between $t = -10$ ms and $t = 0$. Labels show the time elapsed after the rf sweep. The formation of the condensate is reflected by the growth of the central peak.

several traces (Fig. 3B) with the same equilibrium condensate number. Temporal fluctuations of about 20 ms were eliminated by shifting the curves before averaging. The fluctuations in condensate number are probably due to shot-to-shot variations in loading conditions ($\sim 20\%$) and to variations in the truncation caused by drifts of the magnetic field B_0 . Also, because of these fluctuations, there was sometimes a small condensate already produced before the rapid rf sweep. The final condensate fraction varied between 5 and 20%. When no condensate was present right after the rf sweep, the growth started slowly and sped up after 50 to 100 ms. In contrast, if there was already a substantial condensate fraction at the beginning of the rf sweep, rapid growth of the condensate commenced immediately (Fig. 3B). These different behaviors are in agreement with the model based on bosonic stimulation described below.

Because the formation of the condensate is expected to be a Bose-stimulated process, the number of condensate atoms N_0 should grow initially as $\dot{N}_0 = \gamma N_0$, where γ is the initial growth rate. Eventually, when the cloud reaches equilibrium ($N_{0,\text{eq}}$ condensate atoms), the growth rate becomes zero, which can be parameterized by assuming

$$\dot{N}_0 = \gamma N_0 \left[1 - \left(\frac{N_0}{N_{0,\text{eq}}} \right)^\delta \right] \quad (1)$$

The exponent δ was set to $2/5$, consistent

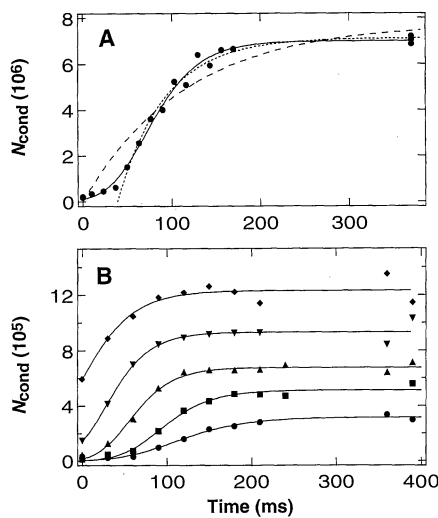


Fig. 3. Growth of the condensate fraction toward equilibrium. Shown is the number of condensate atoms versus the time after the end of the rf sweep. The number of condensate atoms in equilibrium was measured about 400 ms after the rf sweep. (A) Growth of a single condensate in the weak trap (circles); (B) average of about 10 traces with similar equilibrium values for the number of condensate atoms in the strong trap (symbols). The solid lines correspond to the solution of Eq. 1; the dashed and dotted lines in (A) are solutions of Eq. 3.

with an approximate microscopic theory (17) for which the rate of growth is linear in the difference of the chemical potentials of the condensate (which is proportional to $N_0^{2/5}$) and the surrounding thermal cloud. All condensate growth curves in Figs. 3 and 4 were fit with the solution of Eq. 1

$$N_0(t) = N_{0,i} e^{\gamma t} \left[1 + \left(\frac{N_{0,i}}{N_{0,\text{eq}}} \right)^\delta (e^{\delta \gamma t} - 1) \right]^{-1/\delta} \quad (2)$$

The only free parameters were γ and the initial number of condensate atoms $N_{0,i}$ at time $t = 0$, that is, right after the rf sweep. Treating δ as a free parameter did not improve the quality of the fits. Equation 2 describes the observed growth curves very well (Figs. 3 and 4).

It should be pointed out that Eq. 1 is quite different from the differential equation for a pure relaxation process, which is described by

$$\dot{N}_0 = \tilde{\gamma}(N_{0,\text{eq}} - N_0) \quad (3)$$

The solution of Eq. 3 is an exponential approach to equilibrium

$$N(t) = N_{0,\text{eq}}(1 - e^{-\tilde{\gamma}t})$$

that starts right after the rf sweep (dashed line in Fig. 3A); it describes the data very poorly.

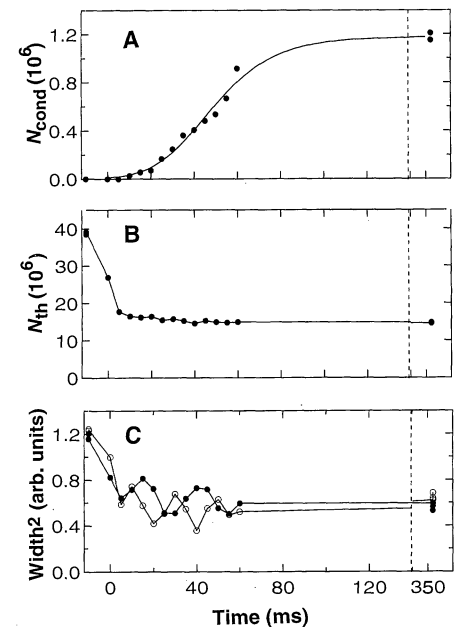


Fig. 4. Initial stage of the formation process, recorded for a single formation event. (A) The number of atoms in the condensate, (B) the number of thermal atoms, and (C) the effective temperature of the cloud, represented by the square of the widths of the thermal cloud in the radial (open circles) and axial (full circles) directions. Note the break in the time axis indicated by the dashed line. The solid line in (A) corresponds to the solution of Eq. 1; those in (B) and (C) connect the data points.

We also added an induction time as an additional free parameter (dotted line in Fig. 3A). With a value of 40 ms, it describes the data fairly well after a small condensate has formed and shows that the main effect of bosonic stimulation is an induction time before the onset of rapid growth. In Eq. 2, this induction time corresponds to the time of pure exponential growth, that is, bosonic stimulation, which is short and prominent only for small N_0 because of the small value of $\delta = 2/5$.

The early stage of condensate formation was studied by taking pictures every 5 ms (Fig. 4). The thermal density showed no major deviation from a Bose-Einstein distribution; the effective temperature quickly relaxed toward half the initial value (Fig. 4C), accompanied by weak, strongly damped quadrupole-type oscillations at a frequency of about two times the axial trap frequency. The total number of thermal atoms reached a quasi-stationary value about 5 ms after the end of the rf sweep and was fairly constant during the formation of the (small) condensate. This quick “equilibration” is in accord with time scales set by the magnetic trap—that is, a quarter cycle in the harmonic potential, which was 3 ms radially and 14 ms axially—and by the elastic scattering rate $\gamma_{el} = n\sigma v \approx 500 \text{ s}^{-1}$; here n is the atom density, $\sigma = 8\pi a^2$ denotes the elastic collision cross section, $v = 4(k_B T/\pi m)^{1/2}$ is the thermal velocity, k_B is the Boltzmann constant, and T is the temperature. Therefore, the condensate growth, which happens on a time scale of 100 ms, should only be weakly perturbed by transients from the initial truncation process. Furthermore, Fig. 3B is evidence that the transients did not suppress the initial condensate growth: the condensate started growing without a notable induction time in those cases where a considerable condensate fraction was already present. These results suggest that condensation occurred in two steps: a fast relaxation that produced an

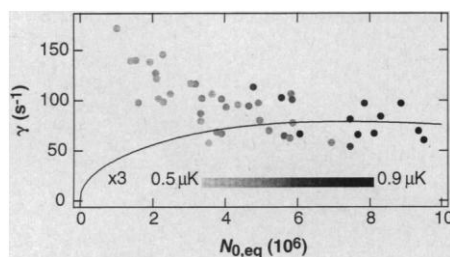


Fig. 5. Condensate growth rate γ versus number of condensate atoms in equilibrium $N_{0,eq}$. The points are fits to single growth curves. The shade of the points indicates the final temperature T of the cloud. $N_{0,eq}$ and T were coupled by the depth of the truncation in the rf sweep. The solid line indicates the theoretical prediction for γ according to Eq. 6, multiplied by a factor of 3.

oversaturated “thermal” cloud, followed by a slower growth of the condensate within the thermal cloud.

A detailed discussion of the second phase of formation has recently been formulated by Gardiner and collaborators (17) for the inhomogeneous Bose gas. They assume that the condensate is in contact with a thermal cloud at a constant temperature below the transition point. Using a master equation based on quantum kinetic theory (17), they derived a growth equation for the condensate (valid for large N_0 , as in our experiment)

$$\dot{N}_0 = 2W^+(N_0) \left\{ \left[1 - \exp\left(\frac{\mu_N - \mu}{k_B T}\right) \right] N_0 + 1 \right\} \quad (4)$$

The first term in the curly brackets is the stimulated scattering term, which is nonvanishing as long as the chemical potential of the thermal bath μ is different from the chemical potential μ_N of the condensate. The last term (the number one) stands for spontaneous scattering into the condensate mode. The function $W^+(N_0)$ is only weakly dependent on N_0 during the formation and, for $\mu \ll k_B T$, is approximately equal to $W^+ = \sqrt{8\zeta(3/2)}\gamma_{el}$, where $\zeta(3/2) \approx 2.612$ is the Riemann zeta function. If we assume μ and $\mu_N \ll k_B T$ in Eq. 4, use a Thomas-Fermi expression for

$$\mu_N = (15\hbar^2 a \sqrt{m\bar{\omega}}^3 N_0 / \sqrt{8})^{2/5} \quad (5)$$

(and similarly for μ , with N_0 replaced by $N_{0,eq}$), and neglect the spontaneous scattering term, we obtain our Eq. 1 with

$$\gamma = 2W^+ \frac{\mu}{k_B T} \propto N_{0,eq}^{2/5} T \quad (6)$$

where $\bar{\omega}$ denotes the geometric mean of the trapping frequencies.

Our results for the rate parameter γ are larger than this theoretical prediction by a factor that ranges between 3 and 15. Furthermore, Eq. 6 predicts an increase of the rate γ with both temperature T and the number of condensate atoms in equilibrium $N_{0,eq}$. The observed trend is in the opposite direction (Fig. 5), that is, γ decreases when $N_{0,eq}$ and T simultaneously increase. This trend is independent of the value assumed for δ between 0.2 and 5 (23). A tentative explanation is saturation of the stimulated growth rate of the condensate. This rate should ultimately be limited by the rate of elastic collisions within the volume of the condensate; strong stimulation would create some local depletion of the thermal cloud, which is not included in the theory.

In order to obtain a full quantitative understanding of the condensate formation,

more detailed studies are necessary experimentally and, especially, theoretically. On the experimental side, an improved signal-to-noise ratio could reveal more clearly the details of the initial phase of condensate formation, dominated by a pure exponential growth, which would provide a direct proof of Bose stimulation. Ultimately, the nucleation process and fluctuations in the onset of condensate formation (9, 14, 16) might be observed. Also, a further characterization of the nonequilibrium situation would be helpful. Theory could include a realistic model of the spatial truncation process, but it seems that a more refined approach is necessary to resolve the discrepancies with our observations.

REFERENCES AND NOTES

- M. H. Anderson, J. R. Ensher, M. R. Matthews, C. E. Wieman, E. A. Cornell, *Science* **269**, 198 (1995); K. B. Davis *et al.*, *Phys. Rev. Lett.* **75**, 3969 (1995); C. C. Bradley, C. A. Sackett, R. G. Hulet, *ibid.* **78**, 985 (1997); see also C. C. Bradley *et al.*, *ibid.* **75**, 1687 (1995).
- M. R. Andrews *et al.*, *Science* **275**, 637 (1997).
- M.-O. Mewes *et al.*, *Phys. Rev. Lett.* **78**, 582 (1997).
- A. Griffin, D. W. Snoke, S. Stringari, Eds., *Bose-Einstein Condensation* (Cambridge Univ. Press, Cambridge, 1995).
- Abstracts from a workshop on Bose-Einstein condensation, Castelvecchio, Italy, 12 to 17 July 1997.
- E. Levich and V. Yakhot, *Phys. Rev. B* **15**, 243 (1977).
- H. T. C. Stoof, *Phys. Rev. Lett.* **66**, 3148 (1991).
- S. G. Tikhodeev, *Sov. Phys. JETP* **70**, 380 (1990) [*Zh. Eksp. Teor. Fiz.* **97**, 681 (1990)].
- H. T. C. Stoof, in (4), pp. 226–245.
- D. W. Snoke and J. P. Wolfe, *Phys. Rev. B* **39**, 4030 (1989); H. Wu, E. Arimondo, C. J. Foot, *Phys. Rev. A* **56**, 560 (1997).
- U. Eckern, *J. Low Temp. Phys.* **54**, 333 (1984); B. V. Svistunov, *J. Moscow Phys. Soc.* **1**, 373 (1991); D. V. Semikoz and I. I. Tkachev, *Phys. Rev. Lett.* **74**, 3093 (1995).
- H. T. C. Stoof, *Phys. Rev. Lett.* **78**, 768 (1997).
- Yu. Kagan, B. V. Svistunov, G. V. Shlyapnikov, *Sov. Phys. JETP* **75**, 387 (1992).
- Yu. Kagan and B. V. Svistunov, *ibid.* **78**, 187 (1994) [*Zh. Eksp. Teor. Fiz.* **105**, 353 (1994)].
- , *Phys. Rev. Lett.* **79**, 3331 (1997).
- Yu. Kagan, in (4), pp. 202–225.
- C. W. Gardiner, P. Zoller, R. J. Ballagh, M. J. Davis, *Phys. Rev. Lett.* **79**, 1793 (1997).
- M.-O. Mewes *et al.*, *ibid.* **77**, 416 (1996).
- W. Ketterle and N. J. van Druten, in *Advances in Atomic, Molecular, and Optical Physics*, B. Bederson and H. Walther, Eds. (Academic Press, San Diego, 1996), vol. 27, pp. 181–236; and references therein.
- E. Hecht, *Optics* (Addison-Wesley, Reading, MA, ed. 2, 1989); M. R. Andrews *et al.*, *Science* **273**, 84 (1996).
- M. R. Andrews *et al.*, *Phys. Rev. Lett.* **79**, 553 (1997).
- G. Baym and C. J. Pethik, *ibid.* **76**, 6 (1996).
- The main effect of changing δ is a change in γ by the inverse factor.
- We thank C. Gardiner and D. Pritchard for stimulating discussions. This work was supported by the Office of Naval Research, the National Science Foundation, the Joint Services Electronics Program (Army Research Office), and the Packard Foundation. D.M.S.-K. acknowledges support from an NSF Graduate Research Fellowship, and H.-J.M. from Deutscher Akademischer Austauschdienst (NATO Science Fellowship).

18 December 1997; accepted 7 January 1997